

In-season Sweetpotato Yield Forecasting using Multitemporal Remote Sensing Environmental Observations and Machine Learning

Mariella Carbajal-Carrasco^{1,2,3}, Daniela Jones^{1,2,4,5}, Cranos Williams^{2,3}, and Natalie Nelson^{1,2,4}

¹Biological and Agricultural Engineering Department, North Carolina State University

²N.C. Plant Sciences Initiative, North Carolina State University

³Electrical and Computer Engineering Department, North Carolina State University

⁴Center for Geospatial Analytics, North Carolina State University

⁵Operations Research and Analysis Group, Idaho National Laboratory

April 26, 2024

2 In-season Sweetpotato Yield Forecasting using Multitemporal Remote 3 Sensing Environmental Observations and Machine Learning

4 Mariella Carbajal-Carrasco^{a,b,e}, Daniela Jones^{a,b,c,d}, Cranos Williams^{b,e}, Natalie Nelson^{a,b,c,*}

5 ^a*Biological and Agricultural Engineering Department, North Carolina State University, Raleigh, NC*

6 ^b*N.C. Plant Sciences Initiative, North Carolina State University, Raleigh, NC*

7 ^c*Center for Geospatial Analytics, North Carolina State University, Raleigh, NC*

8 ^d*Operations Research and Analysis Group, Idaho National Laboratory, Idaho Falls, ID*

9 ^e*Electrical and Computer Engineering Department, North Carolina State University, Raleigh, NC*

10 Abstract

11 Data-driven modeling approaches for crop yield prediction have exponentially increased in the last
12 decade due to the greater availability of spatial data from various sensors. Yet, most yield model-
13 ing has focused on major commodities, leaving lesser-cultivated horticultural crops like sweetpotato
14 relatively undertooled, though these crops considerably contribute to the global economy and food
15 supply. The U.S. is the primary exporter of sweetpotato (271 K tonnes), with 21% of U.S.-grown
16 sweetpotatoes being exported. Early yield forecasting at the county scale offers crucial insights for
17 growers, packers, wholesalers, and associated industries, enabling them to anticipate variations in
18 yield to make informed decisions. While roots and tubers have demonstrated a relationship between
19 yields and above-ground plant characteristics, it remains uncertain whether forecasting models that
20 utilize remotely sensed data, including vegetation indices, are suitable for sweetpotato. We developed
21 county-scale in-season sweetpotato yield forecast models using machine learning (ML) algorithms and
22 multitemporal remote sensing environmental data. Four of the most commonly used ML algorithms
23 for predicting crop yield - Random Forest Regression (RFR), Artificial Neural Networks (ANN), Sup-
24 port Vector Machine (SVM), and Extreme Gradient Boosting (XGB) - were applied using stationary
25 (topography and soil characteristics), and temporal (weather, NDVI, and Growing Degree Days)
26 variables as potential predictors. Six predictor sets were tested to identify key predictor variables,
27 optimal aggregation time (16 or 32 days composite) of the temporal variables, and how early in the
28 growing season the models can reliably predict end-of-season yields. U.S. Annual CropScape land
29 cover layers were used to identify sweetpotato fields, over which temporal variables were aggregated,
30 and sweetpotato yields were tabulated from the USDA Agricultural Survey from 2008 to 2022. The
31 Boruta method was used for feature selection across each predictor set before training the ML models.
32 RFR outperformed other ML algorithms and the RFR models' evaluation metrics were the most con-
33 sistent across the six predictor sets. The RFR model that incorporated early and mid season temporal
34 variables as 16-day composites was selected and proposed for future sweetpotato yield forecasting due
35 to its performance ($R^2 = 0.44$, $RMSE = 3.53 \text{ tonnes.ha}^{-1}$), as well as ability to predict early enough

36 in the season to provide actionable information. In the final model, several stationary variables (el-
37 evation, nitrogen, cec, soc, and clay content) were the most predictive of sweetpotato yield. After
38 these stationary variables, NDVI and precipitation from the time around storage root initiation and
39 bulking (July), and minimum temperature around planting (June) followed in importance.

40 *Keywords:* Random forest, XGBoost, neural networks, yield prediction model, vegetation index,
41 NDVI, Sentinel-2, Landsat

42 1. Introduction

43 Innovations in technology and access to remote sensing data have driven huge advances in the
44 application of artificial intelligence to agriculture, such as to predict yields (Jung et al., 2021). In
45 particular, machine learning (ML) algorithms are effective at crop yield prediction due, in part, to
46 their ability to use observational data and measurements across several experiments. Additionally,
47 non-linear ML algorithms do not assume a defined pattern (i.e. linear, polynomial) between the
48 predictor and response variables and can account for non-linear relationships evident through patterns
49 in recorded data (Paudel et al., 2022), making them well suited for use with agricultural observations.
50 Even though ML models are unable to explain underlying processes, they can surpass the predictive
51 accuracy of process-based models (Leng and Hall, 2020), making ML algorithms particularly useful
52 for yield forecasting at scales that are often computationally prohibitive for process-based models.
53 Artificial Neural Networks and Random Forest Regression are among the most used and successful
54 ML algorithms for predicting crop yield, specifically using agroclimatic variables derived from remote
55 sensing products as predictors (Van Klompenburg et al., 2020).

56 While ML-based yield forecasting has become increasingly common, most yield forecasting re-
57 search has predominantly concentrated on field-scale predictions (Van Klompenburg et al., 2020).
58 These forecasts are highly site-specific and less suitable for extrapolation to other fields. A few stud-
59 ies have put forth crop yield prediction models at the county scale, but only for major crops - e.g.,
60 wheat, corn and soybean (Cao et al., 2021; Zhou et al., 2022; Kang et al., 2020; Ghazaryan et al.,
61 2020) - leaving growers of non-major commodities without forecast information to inform farm man-
62 agement. Moreover, it is unclear whether existing forecasting frameworks that work effectively for
63 crops like wheat, corn and soybean will transfer to other crops with distinct physiology, like roots and
64 tubers. Although roots and tubers grow underground, studies suggest a relationship between yield
65 and above-ground traits, such as vegetation indices or canopy cover, particularly during vegetative
66 growth and around tuber or storage root initiation (Tedesco et al., 2021; Pérez-Pazos et al., 2021;

*Corresponding author

Email address: mnelson4@ncsu.edu (Natalie Nelson)

67 Sun et al., 2020). The relationship between yields and above-ground plant characteristics indicates
68 that remotely sensed data may still be useful when predicting root and tuber yield.

69 Among yield forecasting studies focused on roots and tubers, greater attention has been dedicated
70 to potato. Prior potato forecasting studies have demonstrated that high-resolution vegetation bands
71 and indices (from UAV or Sentinel-2) acquired during full vegetative growth and around tuber initi-
72 ation were predictive of potato yield, at both field (Sun et al., 2020; Gómez et al., 2019) and regional
73 scales (Salvador et al., 2020). Additionally, tuber set was better predicted than tuber yield due to
74 its higher correlation with above-ground biomass monitored with spectral data (Sun et al., 2020).
75 Furthermore, studies that incorporated more precise in-situ data, such as cultivar information (e.g.,
76 plant height) (Li et al., 2021) or soil characteristics, along with proximal data (Abbas et al., 2020)
77 during the growing season, achieved higher prediction performance.

78 In contrast to potato, ML-based forecasting models have not yet been tested or developed for
79 sweetpotato. The complex interplay of multiple genotype traits, phenological dynamics, and envi-
80 ronmental factors in sweetpotatoes across tropical and some temperate regions, along with limited
81 availability of in-season data, poses challenges for accurately predicting sweetpotato yield. Despite
82 the lack of attention sweetpotato has received from yield forecasters, sweetpotato is a key crop in
83 regions of the United States of America (USA), which is the primary exporter of sweetpotato globally.
84 In 2021, the USA exported 271 K tonnes of sweetpotatoes (USDA National Agricultural Statistics
85 Service, 2022b). Within the USA, North Carolina (NC) is the largest sweetpotato-producing state,
86 generating nearly half of the national sweetpotato supply and having influence on national (Soto-
87 Caro et al., 2022) and international markets. Having access to a sweetpotato forecasting model
88 would help growers, packers, wholesalers, and supporting businesses (e.g., exporters, crop insurers)
89 have information with which to anticipate and respond to yield deviations.

90 While a sweetpotato forecasting model does not yet exist, prior studies have tested ML algorithms
91 for predicting other aspects of sweetpotato production. Villordon et al. (2009a) evaluated eight
92 growing degree day (GDD) calculation methods with three base temperatures (60, 65 and 70 F), five
93 ceiling temperatures (80, 85, 90, 95, 100 F), and six machine learning algorithms (support vector
94 machine, multivariate adaptive regression, neural networks, linear regression, regression tree, and
95 generalized linear model) to identify suitable models for predicting optimal harvest dates. Then,
96 Villordon et al. (2010) used a Bayesian Belief Network (BBN) approach to identify the agroclimatic
97 variables known to influence critical storage root initiation in marketable sweetpotato yield. Similarly,
98 Villordon et al. (2011) used a BBN and data on agroclimatic conditions to determine the optimal
99 in-row spacing to reach the highest marketable yield. Combined, these studies demonstrate the
100 importance of optimum air and soil temperatures during storage root formation, insights on which
101 can be used towards developing a sweetpotato yield forecasting model.

102 In this study, we developed county scale in-season sweetpotato yield forecast models using ML
103 algorithms and multi-temporal remote sensing, and environmental data. Specifically, our objectives
104 were to (1) identify key predictor variables through feature selection from candidate variables includ-
105 ing Normalized Difference Vegetation Index (NDVI), maximum temperature, minimum temperature,
106 precipitation, GDD, topography, and soil properties, (2) implement four ML algorithms, specifi-
107 cally Random Forest Regression (RFR), Artificial Neural Networks (ANN), Support Vector Machine
108 (SVM), and Extreme Gradient Boosting (XGB), to predict in-season sweetpotato yields at the county
109 scale, (3) determine the optimal aggregation periods for temporal predictor variables, and (4) eval-
110 uate how early in the growing season models are able to reliably predict end-of-season yields. We
111 focused on North Carolina (NC; USA) counties in and around the Coastal Plain agro-region, where
112 the highest sweetpotato production occurs in the state.

113 **2. Materials and methods**

114 *2.1. Study area*

115 We focused on NC counties with reported sweetpotato production (USDA National Agricultural
116 Statistics Service, 2022b) from 2008 to 2022 (Figure 1), which comprises major sweetpotato producers
117 and exporters. The majority of the counties were located in the Rolling Coastal Plains (Level IV) and
118 Southeastern Plains (Level III) ecoregions (Griffith et al., 2002), where environmental conditions are
119 ideal for sweetpotato growth. All counties for which yield data (ranging between 12.55 to $33.89 t.ha^{-1}$)
120 and predictor variables ($n = 17$) were available were considered in this analysis. These counties are
121 outlined in Figure 1 and included: Johnston, Sampson, Chowan, Edgecombe, Harnett, Nash, Wake,
122 Wayne, Wilson, Robeson, Duplin, Lenoir, Pitt, Columbus, Martin, Lee, and, Moore. To narrow
123 down the location of sweetpotato fields within each county, counties were also matched with gridded
124 sweetpotato areas classified by the Cropland Data Layer (CDL, 30-m resolution), hosted in the web-
125 based tool CropScape (USDA National Agricultural Statistics Service, 2022a). CDL was used to
126 identify sweetpotato harvested areas every year (pixel code: 46). Figure 2 depicts how sweetpotato
127 harvested areas nearly doubled from 2008 ($120 km^2$) to 2022 ($229 km^2$). Figure 2 also illustrates the
128 concentration of sweetpotato fields within the studied counties.

129 *2.2. Modeling approach*

130 Crop yield is driven by interactions between genetics, environment, and management (Gajanayake
131 et al., 2014). When developing a crop yield forecasting model for use across a region, only environ-
132 mental variation can be directly accounted for, as genetics and management will vary by farm. While
133 genetic and management data cannot be included in a model designed for regional application, the

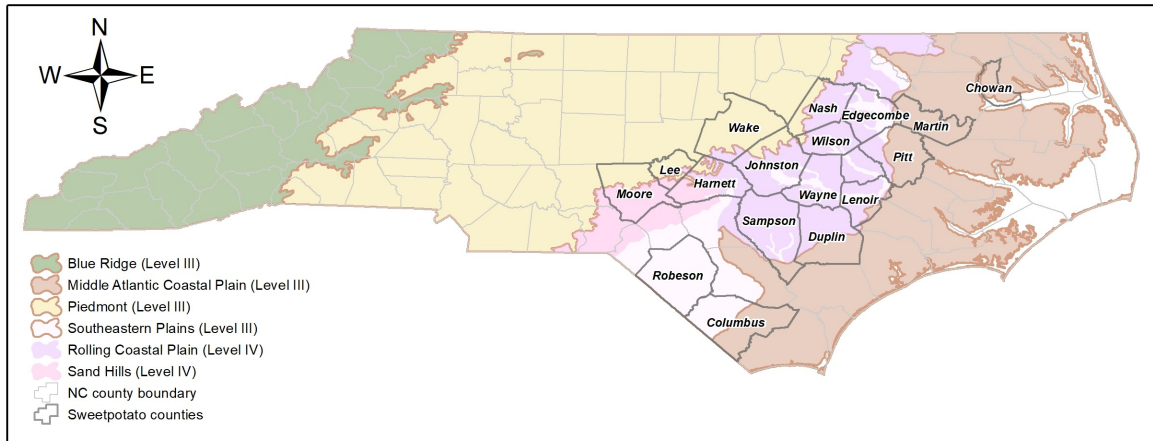


Figure 1: North Carolina counties that reported sweetpotato harvested areas and yield in USDA Statistics (USDA National Agricultural Statistics Service, 2022b) from 2008 to 2022

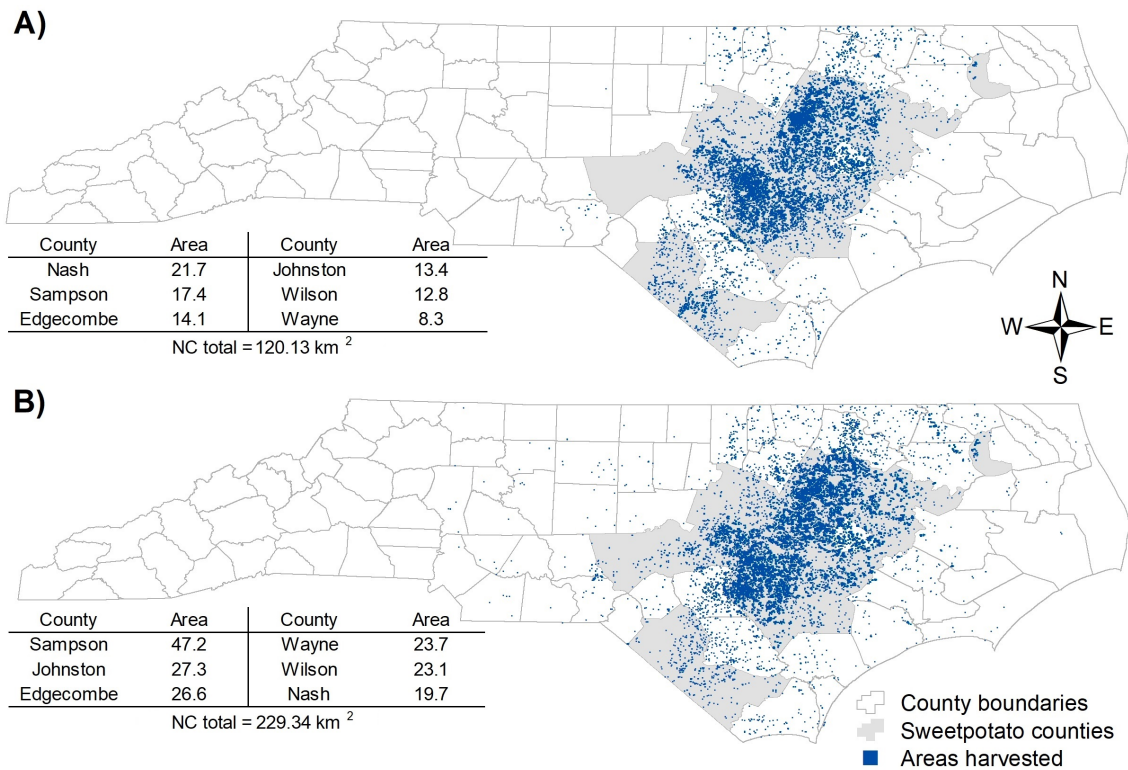


Figure 2: Sweetpotato harvested areas (km^2) in A) 2008 and B) 2022 derived from the Cropland Data Layer (CDL) (USDA National Agricultural Statistics Service, 2022a). Counties with gray fill have reported sweetpotato yields from USDA NASS. Colored pixels show sweetpotato fields reported in the CDL; pixels are magnified for visualization purposes. The table in each panel summarizes the CDL top six counties in terms of areas harvested, as well as the total harvested area across NC

134 characteristics of common genotypes and management practices can inform the selection and sum-
135 mary of candidate predictor variables. Here, we considered both stationary (i.e., topography and soil)
136 and temporally varying (i.e., weather and vegetation greenness) variables as predictors, and evaluated
137 which predictors and aggregation periods were associated with optimal model performance.

138 To determine the optimal modeling framework, we tested different combinations of predictor
139 variable sets that included all of the stationary variables, as well as temporal variables divided into
140 different growing season stages including: (1) only the early season (referred to as "early"), (2) the
141 early and mid season (referred to as "early-mid"), and (3) the early, mid, and late season (referred
142 to as "early-late").

143 To estimate the dates corresponding to the different growing season stages, we used Covington
144 as our target cultivar as it accounts for 85-90% of sweetpotato production in NC (Yencho et al.,
145 2008). Togari (1950) defined early, middle and late thickening stages occurring up to 25 days after
146 transplanting (DAT), from 25 to 60 DAT, and from 60 DAT to harvest, respectively. Similarly,
147 Villordon et al. (2009b) found that visible storage root initiation occurs around 26 DAT. Additionally,
148 Covington has a maturity time of 90 to 120 days (Yencho et al., 2008), and most sweetpotato slips in
149 NC are transplanted from early May through late June (Meyers et al., 2014) and harvested from late
150 August through early November (NC State Extension, 2017). Thus, June 1st could be considered as
151 the average planting date across NC counties. Accordingly, in this study, the early season was defined
152 as spanning June 1st to July 2nd (0 to 32 DAT), the mid-season as July 3rd to August 3rd (33 to 65
153 DAT), and the late season as August 4th to September 4th (66 to 96 DAT).

154 The early and early-mid models are those that could be used for in-season forecasting; i.e., the
155 early season model could be run as early as July 2nd (before the first day of the mid-season) and
156 the early-mid season model could be run as early as August 3rd. The late season model could not
157 be used for in-season forecasting, since it could only be run on September 4th, which is too close
158 to harvest so as to provide advance yield predictions. However, the early-late season model was
159 included in this assessment for comparison purposes, particularly since we assume that late-season
160 values (e.g., of NDVI) are more predictive of yields at harvest given that they capture conditions
161 observed immediately before harvest.

162 Additionally, we tested two different composite periods for the temporal variables: 16-days and
163 32-days; these time periods were determined based on the temporal resolution of the satellite remote
164 sensing data used to estimate vegetation greenness (described below). Thus, in total, there were
165 6 different predictor variable sets that were screened (3 based on the season times and 2 based on
166 temporal variables).

167 *2.3. Datasets and preprocessing*

168 To create a generalizable model framework, we considered only predictors for which publicly
 169 available spatial datasets were available over our study period of 2008 to 2022. Annual county-scale
 170 sweetpotato yields reported by the USDA Survey (USDA National Agricultural Statistics Service,
 171 2022b) was the response variable, and predictors were averaged over each county. We also compared
 172 the total harvested sweetpotato area reported at the county- and state-scale by the USDA Survey
 173 (annual), Census (every 5 years), and CDL (annual) to assess agreement between the datasets and
 174 identify potential bias. Because the USDA Census only occurs every 5 years, we could only consider
 175 Census data from 2012 and 2017. 2008 was chosen as the initial study year because sweetpotato was
 176 not included in the CDL prior to 2008.

177 As candidate predictor variables (Table 1), we considered topography and soil characteristics,
 178 which were temporally stationary, and precipitation, maximum and minimum temperature, GDD
 179 and NDVI as temporally variant predictors.

Table 1: Environmental variables used as candidate predictors in the machine learning models for sweetpotato yield forecast

Type	Variable	Source	Resolution
Stationary	Elevation (m.)	STRM V4 - CGIAR ¹	90 m.
	Slope		
	Aspect		
	Sand (%)	SoildGrids 2.0 - ISRIC ²	250 m.
	Clay (%)		
	pH		
	Cation Exchange Capacity		
Bulk density	PRISM - Climate Group ³	4638.3 m.	
Nitrogen			
Soil Organic Carbon			
Temporal	Precipitation (mm.)	Landsat 5, 7, 8 ⁴ / Sentinel-2 - NASA ⁵	30 m.
	Maximum temperature (°C)		
	Minimum temperature (°C)		
Target	Yield (t/ha)	USDA Statistics ⁶	county

¹ Jarvis et al. (2008), ² Poggio et al. (2021), ³ PRISM Climate Group, Oregon State University (2022),

⁴ <https://landsat.gsfc.nasa.gov/>, ⁵ <https://sentinel.esa.int/web/sentinel/missions/sentinel-2>,

⁶ <https://quickstats.nass.usda.gov/>

180 *2.3.1. Stationary predictor variables: Topography and soil*

181 Topography and soil characteristics were assumed to be stationary over the study period. For
 182 topography variables, digital elevation data (DEM) from the Shuttle Radar Topographic Mission
 183 (SRTM), produced by NASA and improved by the Consortium for Spatial Information (CGIAR-
 184 CSI) (Jarvis et al., 2008), was used to get elevation (m.), and derived to slope (°) and aspect (°)
 185 using the ee.Terrain.slope and ee.Terrain.aspect functions, respectively, from Google Earth Engine
 186 (GEE). Soil characteristics such as sand (%), clay (%), pH (phh2o), cation exchange capacity (cec,
 187 $cmol(c).kg^{-1}$), bulk density (bdod, $kg.dm^{-3}$), nitrogen ($g.kg^{-1}$), and soil organic carbon ($soc.g.kg^{-1}$)

188 at 5 - 15 cm depth from SoilGrids (Poggio et al., 2021), a global gridded soil information database
 189 that accounts for multiple soil characteristics at different depth ranges, were also included as predictor
 190 variables.

191 *2.3.2. Temporal predictor variables: Weather and vegetation greenness*

192 When summarizing the variables, we used a naming convention of the variable’s abbreviation and
 193 composite start date; for instance, tmin_06-01 corresponds to the mean daily minimum temperature
 194 for the composite starting on June 1st until either June 16th or July 2nd, depending on the time
 195 aggregation or composite (i.e., 16- or 32-days).

196 In-season weather was accounted for using daily precipitation (ppt, mm.), and maximum (tmax,
 197 °C) and minimum temperature (tmin, °C) from the PRISM (Parameter-elevation Regressions on
 198 Independent Slopes Model) Daily Spatial Climate Dataset AN81d (PRISM Climate Group, Oregon
 199 State University, 2022), developed by the PRISM Climate Group at Oregon State University. In
 200 addition, GDD (i.e., the heat accumulation that contributes to crop growth and development) was
 201 calculated according to Equation 1 (Dufault, 1997). This equation was used based on Villordon et al.
 202 (2009a), who found that it was the more accurate GDD formulation for predicting sweetpotato yields.

$$GDD = \begin{cases} 0, & \text{if } T_{min} < B \\ C - B, & \text{if } T_{min} \geq B \text{ and } T_{max} > C \\ T_{max} - B, & \text{if } T_{min} \geq B \text{ and } T_{max} \leq C \end{cases} \quad (1)$$

203 In Equation 1, T_{max} and T_{min} are the daily maximum and minimum temperatures, respectively.
 204 B is the base temperature for total biomass production, defined as 16.9 °, and C is the ceiling tem-
 205 perature, defined as 29.2 ° (Gajanayake et al., 2014). Daily precipitation and GDD were summed to
 206 create totals, whereas daily maximum and minimum temperatures were averaged for every composite
 207 period.

208 NDVI was included as a proxy of crop health and growth, as well as a measure of unmonitored
 209 management practices (e.g., agrochemical application). Although sweetpotato grows underground,
 210 studies on other roots and tubers (including sweetpotato) report a correlation between storage root
 211 biomass and canopy growth and development, especially from root establishment to maximum canopy
 212 expansion (Tedesco et al., 2021). NDVI is the most widely-used metric for quantifying the health
 213 and density of vegetation, and it is calculated from red and near-infrared light surface reflectance
 214 (Equation 2). NDVI ranges from -1 to 1, where 1 corresponds to more dense and healthy vegetation,
 215 positive values close to 0 correspond to no vegetation (i.e., bare soil or urban areas), and negative
 216 values correspond to the presence of water.

$$\text{NDVI} = \frac{\text{NIR} - \text{Red}}{\text{NIR} + \text{Red}} \quad (2)$$

217 NDVI was calculated from different satellites (Landsat series and Sentinel-2) and sensors to max-
 218 imize data availability (Table 2). The 16- and 32-day aggregation periods for the temporal input
 219 variables were defined because of the Landsat revisit time. Building an NDVI time series using dif-
 220 ferent sensors with different spectral ranges requires a harmonization process of either the surface
 221 reflectances or NDVI (Chastain et al., 2019; Villaescusa-Nadal et al., 2019; Zhang et al., 2018; Roy
 222 et al., 2016), or an equivalent atmospheric correction that allows for the intercomparison of sur-
 223 face reflectances across sensors (Yin et al., 2019). Thus, even though Sentinel-2 top-of-atmosphere
 224 (TOA) provided a longer period of available images (from 2015), the harmonization process of the
 225 atmospherically-corrected surface reflectance (bottom-of-atmosphere, BOA) was preferred due to its
 226 use requiring considerably less processing time.

Table 2: Sensors characteristics used for calculating NDVI time series. *Note that spatial resolution is for Red and NIR bands only.

Satellite and sensor	Spatial resolution* (m.)	Revisit time (days)	Red band, band range (nm)	NIR band, band range (nm)	Years used
Sentinel-2 MSI	10	5	B4 (650 - 680)	B8 (785-900)	2019 - 2022
Landsat 8 OLI	30	16	SR_B4 (640 - 670)	SR_B5 (850 - 880)	2013 - 2018
Landsat 7 ETM+	30	16	SR_B3 (630 - 690)	SR_B4 (770 - 900)	2012
Landsat 5 TM	30	16	SR_B3 (630 - 690)	SR_B4 (760 - 900)	2008 - 2011

227

228 Table 2 summarizes the Landsat (OLI, ETM+, TM) and Sentinel-2 (MSI) level 2 products used
 229 for the study time frame, as well as the spectral, spatial and temporal resolutions considered when
 230 calculating the NDVI time series. First, preprocessing included the conversion of Digital Numbers
 231 (DNs) to surface reflectance (scaled from 0 to 1). DNs from Landsat surface reflectance bands
 232 (collection 2) were converted to surface reflectance by multiplying pixel values by 0.0000275 and
 233 subtracting 0.2 (U.S. Geological Survey, 2023). Similarly, DNs from the Harmonized Sentinel-2 MSI
 234 were multiplied by 0.0001. Afterwards, pixels with questionable data (e.g. clouds) were masked using
 235 their corresponding pixel quality band. In addition, pixels with missing values were filled using a
 236 square kernel radius of 1 pixel. This algorithm was iterated four times for Sentinel-2, Landsat TM
 237 and OLI, and 10 times for Landsat ETM+ in order to account for the black strips caused by the
 238 Scan Line Corrector (SLC) failure in 2003. Then, NDVI was calculated using Equation 1 and all
 239 images found in every time composite were aggregated by the maximum NDVI pixel value. Finally,
 240 NDVI values calculated from Landsat were harmonized to Sentinel-2 using ordinary least squares
 241 (OLS) regression coefficients shown in Table 3. The 16-day composite starting on August 4th, 2011,
 242 (ndvi_08-04) was removed due to suspiciously low NDVI values, suspected to be due to cloud cover.
 243

Table 3: Ordinary least squares (OLS) regression coefficients to harmonized NDVI values calculated from surface reflectance images from Landsat and Sentinel-2.

Sensor	Intercept	Slope	Reference
TM / ETM+ to OLI	0.0235	0.9723	Roy et al. (2016)
OLI to MSI	0.0016	1.0016	Zhang et al. (2018)

2.3.3. Preprocessing

Yearly stationary and temporal input variables were preprocessed in the Google Earth Engine (GEE) Code Editor, an open-source cloud computing platform designed to access and analyze geospatial data. Temporal input variables followed the initial preprocessing as described in Section 2.3.2. Afterwards, all stationary and temporal potential predictors (described above) were masked such that only pixels overlapping with sweetpotato harvested areas identified by CDL were considered in the analysis, and values were then spatially averaged per county. Finally, predictors and target variable yield datasets were merged, resulting in a total of 95 records given that not all 17 counties reported yields for sweetpotatoes in the 14 years of study.

2.4. Machine learning models

ML models can handle a large number of predictors. However, including potential predictors that are redundant or not important can cause overfitting or a decrease in model performance (Khan et al., 2020). Among the various feature selection approaches that exist, the Boruta algorithm (Kursa et al., 2010), a method based on the Random Forest algorithm for identifying all relevant variables, was chosen because of its effectiveness working with remotely sensed agricultural data (Fei et al., 2022; Keskin et al., 2019). While the Boruta method is based on the Random Forest algorithm, its feature selection results are broadly applicable for use with other machine learning algorithms. In the Boruta method, the variable importance of a feature is measured by calculating the average loss of its accuracy divided by the standard deviation of all losses (Z-score) with reference to that of the shadow attributes (a randomized copy of the system variables) (Kursa et al., 2010; Kursa and Rudnicki, 2010). The Boruta method assigned predictors as relevant, tentative, and non-relevant. The tentative attributes were reanalyzed and forced to be classified as relevant or not relevant.

Feature scaling is also a key transformation in an ML pipeline since predictor variables are in different units and scales, and can cause discrepancies affecting model performance and variable importance scores. There are several scaling methods like minimum-maximum normalization and standardization; however, they can impact model performance differently (Ahsan et al., 2021). Even when tree-based algorithms do not need feature scaling because model performance is not affected, neglecting to scale predictors can affect variable importance measures (Strobl et al., 2007; Balabaeva and Kovalchuk, 2019). Therefore, the most common and successfully scaling methods - minimum-maximum normalization, standardization, and standardization combined with the YeoJohnson method - were

274 evaluated, and the one that produced the best model performance was chosen for each model.

275 For the ML implementation approach, four of the most commonly used ML models for yield
276 forecasting reported in literature (Cao et al., 2021; Van Klompenburg et al., 2020) - RFR, ANN,
277 SVM, and XGB - were trained, tuned, tested and compared. After feature selection, the dataset was
278 partitioned into 5-folds based on the response variable, and every model was trained and tested five
279 times, using four folds for training and one fold for testing. Then, hyperparameter tuning employed
280 a 10-fold cross-validation technique repeated 3 times, which is especially useful and robust for small
281 datasets. Each model hyperparameters were manually tuned for each ML algorithm. The overall
282 model performance was determined by computing the average metrics over the 5-fold.

283 Finally, a model based on all data (without partitioning) and the best-performing algorithm was
284 trained, and the most important predictor variables affecting sweetpotato yield predictions were
285 analyzed.

286 Model training, tuning, and testing were implemented in R (R Core Team, 2023) and RStudio
287 (RStudio Team, 2021) using the Boruta (Kursa and Rudnicki, 2010), caret (Kuhn and Max, 2008),
288 randomForest (Liaw and Wiener, 2002), nnet (Venables and Ripley, 2002), and xgboost (Chen and
289 Guestrin, 2016) packages.

290 2.5. Model Evaluation Metrics

291 The performances of the ML models were evaluated using the root mean squared error (RMSE,
292 Equation 3) and R squared score (R^2 , Equation 4). The RMSE quantifies the difference between
293 predicted values and actual values in the same target units, and the R^2 represents the proportion of
294 variance explained by the model (Chicco et al., 2021). RMSE was indicated as the optimizer metric
295 during the training process.

$$RMSE = \sqrt{\frac{1}{n} \sum_{i=1}^n (y_i - \hat{y}_i)^2} \quad (3)$$

$$R^2 = 1 - \frac{\sum_{i=1}^n (y_i - \hat{y}_i)^2}{\sum_{i=1}^n (y_i - \bar{y})^2} \quad (4)$$

296 In Equations 3 and 4, n is the number of data points, y_i is the observed value for the i -th data
297 point, \hat{y}_i is the predicted value for the i data point, and \bar{y} is the mean of the observed values y_i .

298 3. Results

299 3.1. Consistency between USDA CDL, Survey and Census data

300 Prior to training and testing forecast models, the harvested areas of sweetpotato were evaluated
301 across the USDA CDL, Survey, and Census. Since the CDL was used for data preprocessing, but the

302 Survey yield data were used as training data for the response variable, we wanted to ensure there was
 303 reasonable consistency between the datasets with regards to their shared variable, harvested area.
 304 The comparison of annual sweetpotato harvested areas estimated by CDL with respect to the USDA
 305 Survey data (Figure 3) showed a high agreement between 2008 to 2016, with 26% more harvested
 306 areas reported by the Survey than the CDL on average. Conversely, from 2017 to 2022, CDL had a
 307 very low agreement with NASS Survey data between 2017 to 2019, reporting on average 103% more
 308 harvested area than the Survey data, and a very good agreement between 2020 to 2022, with an
 309 average 13% increase in area reported by CDL than the Survey. In addition, when comparing with
 310 USDA Census data, both CDL and survey data estimated 26% less harvested areas in 2012; and 1.7%
 311 more and 43% less harvested areas, respectively, in 2017.

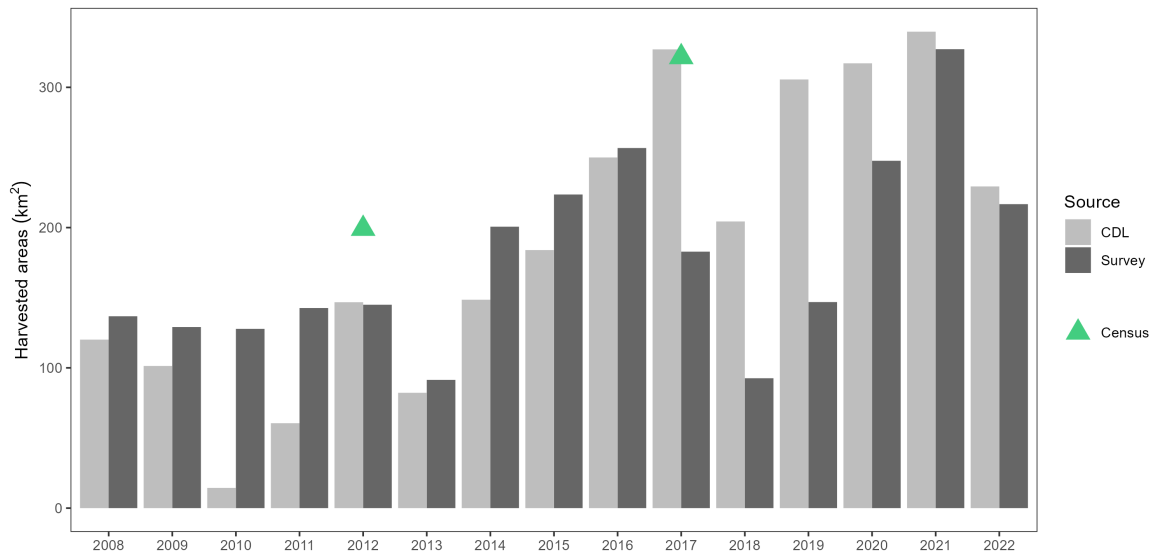


Figure 3: Sweetpotato harvested areas reported by Crop Data Layer (CDL) (USDA National Agricultural Statistics Service, 2022a), Quick Stats and the Census of Agriculture (USDA National Agricultural Statistics Service, 2022b) during the time frame of study

312 The CDL and Survey data were compared with Census data at the county scale, and trend lines,
 313 which intersected at zero, were fitted, resulting in line slopes of 0.93 (CDL vs. Census) and 0.58
 314 (Survey vs. Census) in 2012, and 0.76 (CDL vs. Census) and 0.76 (CDL vs. Census) in 2017 (Table
 315 4). Top producing counties were similar for all data sources in both years; therefore, CDL and Survey
 316 data had high correlation ($R^2 \geq 0.88$) when compared with Census data. The agreement between
 317 CDL and Survey data provided support to the utilization of CDL data for preprocessing predictors
 318 and Survey data as the model's true target yield.
 319

320 3.2. Feature selection

321 The Boruta feature selection applied to the six predictor sets showed the same top three most
 322 important variables - elevation, nitrogen and cec - and somewhat less important variables, soc and

Table 4: Comparison of the sweetpotato harvested areas per county reported by Census, Survey and Crop Data Layers (CDL on Census of Agriculture years (2012 and 2017). Descending ordered from Census data. Showing only harvested areas $> 1km^2$

2012				2017			
County	Census	Survey	CDL	County	Census	Survey	CDL
Johnston	43.05	37.64	20.63	Nash	62.74	39.13	32.18
Nash	41.59	37.84	24.33	Johnston	60.17	43.71	40.74
Sampson	37.35	36.22	25.64	Sampson	55.50		54.32
Wilson	27.73	28.13	16.13	Wilson	45.41	39.26	36.73
Wayne	11.04		7.08	Edgecombe	17.13	34.28	26.90
Columbus	10.23		3.35	Wayne	15.37		27.64
Edgecombe	6.35		7.88	Duplin	14.36	13.76	12.93
Duplin	6.22		7.51	Harnett	12.57		9.43
Harnett	4.77	5.18	3.08	Wake	11.25		2.83
Pitt	4.74		4.91	Columbus	9.64		5.18
Robeson	2.57		2.14	Lenoir	6.34	11.13	11.31
Wake	2.48		1.45	Robeson	5.09		3.02
Chowan	1.09			Pitt	4.41		16.96
Cumberland			3.38	Lee	0.98		
Greene			9.63	Moore	0.68		
Lenoir			5.44	Martin		1.58	1.55
				Bertie			3.93
				Halifax			3.53
				Cumberland			3.29
				Scotland			1.33
				Bladen			1.24
				Greene			23.43
Total	199.19	145.00	142.58	Total	321.63	182.84	318.47
Slope		0.93	0.58	Slope		0.76	0.76
R^2		1.00	0.96	R^2		0.91	0.88

323 clay (Figure 4). Consistently, all predictor sets had similar variables following the top three most
324 important variables, which were temporally variant variables including NDVI and GDD at specific
325 time points in the mid-season. However, the specific time points corresponding to important predictors
326 varied depending on the data configuration. Figure 4 illustrates variable importance along with the
327 final classification of variables (unimportant, important) for early-mid predictor sets (16- and 32-days
328 composites).

329 3.3. Model performance and selection of final model

330 The 5-fold average metrics (Table 5) showed that RFR consistently outperformed other ML algo-
331 rithms. The best model was selected based on the R^2 and RMSE from the testing data, prioritizing
332 the early and early-mid season models over late season models given their ability to provide in-season
333 forecasts well ahead of harvest. Thus, the early-mid season with 16-day aggregation had the best
334 testing (RMSE = $3.53 t.ha^{-1}$, $R^2 = 0.44$) performance, which was exactly the same as the early-late
335 model.

336 XGB performed very similar or even slightly better than RFR during both training and testing,
337 but only when temporal variables included data through the late season. However, when temporal
338 variables included data only up to the early or mid season, XGB performance decreased and fell below

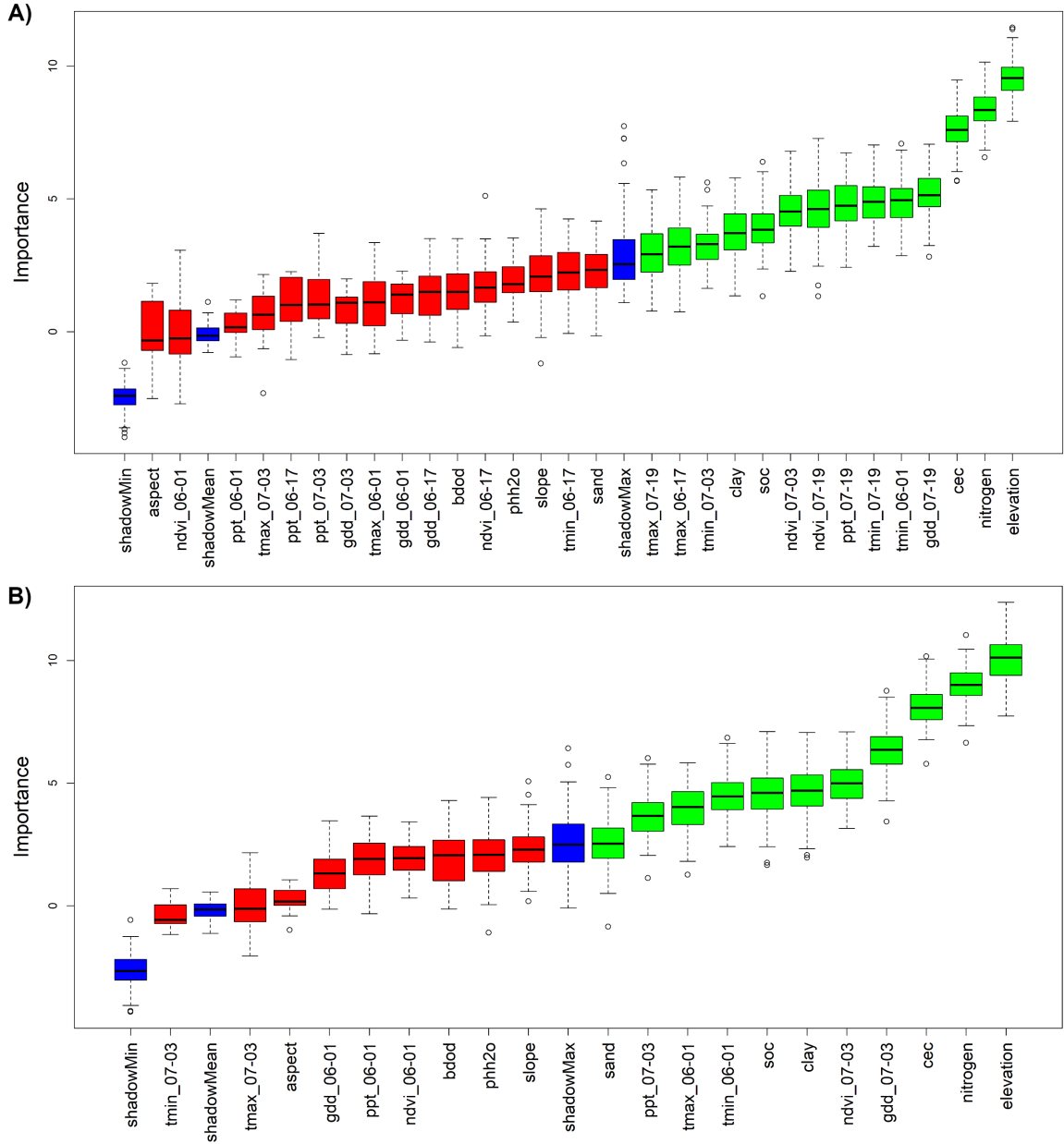


Figure 4: Importance of all potential predictors, determined by the Boruta Feature selection method for stationary and temporal variables until Mid season (June - July) with A) 16-days and B) 32-days time composites. Where, the most important variables are in green, the least important variables are in red, and the threshold variables are in blue. See Supplementary Materials for Early (June) and Late (June - August) seasons.

339 that of RFR.

Table 5: Model performance, Root Mean Square Error (RMSE, $t.ha^{-1}$) and R^2 , of county-level sweetpotato yield forecast for different ML algorithms, input time composites and season. ML models Random Forest (RFR), Artificial Neural Networks (ANN), Support Vector Machine (SVM), and eXtreme Gradient Boosting (XGB) were applied using stable and temporal variables until late (June - August) and Mid (June - July) season, with 16-days and 32-days time composites.

Composite	Season	Model	Training		Testing	
			RMSE	R^2	RMSE	R^2
16-days	early -late	RFR	1.58	0.89	3.52	0.44
		ANN	2.47	0.72	3.92	0.29
		SVM	2.90	0.62	4.02	0.27
		XGB	1.25	0.92	3.53	0.43
	early - mid	RFR	1.58	0.89	3.53	0.44
		ANN	2.67	0.68	3.94	0.30
		SVM	2.85	0.63	4.11	0.23
		XGB	1.10	0.93	3.77	0.36
	early	RFR	1.70	0.87	3.77	0.36
		ANN	3.49	0.46	4.33	0.15
		SVM	3.02	0.58	4.30	0.14
		XGB	1.98	0.78	4.04	0.26
32-days	early -late	RFR	1.61	0.88	3.53	0.44
		ANN	2.77	0.65	3.92	0.31
		SVM	2.91	0.61	4.05	0.25
		XGB	1.23	0.89	3.46	0.46
	early - mid	RFR	1.68	0.87	3.67	0.39
		ANN	3.27	0.52	4.18	0.21
		SVM	3.05	0.58	4.44	0.10
		XGB	2.18	0.79	3.49	0.44
	early	RFR	1.66	0.88	3.65	0.4
		ANN	3.40	0.49	4.27	0.17
		SVM	3.32	0.51	4.40	0.12
		XGB	1.87	0.8	3.71	0.38

340

341 Considering both performance and ability to be used as an in-season forecasting model, the RFR
342 algorithm built with early-mid season predictors aggregated at 16-days was selected as the "best"
343 model and further analyzed. Due to the small dataset, a final RFR model was trained without data
344 partitioning using out-of-bag (OOB) cross validation to maximize the amount of data available for
345 model training. The final model's OOB error was $RMSE = 3.64 t.ha^{-1}$ with a $R^2 = 0.41$. The
346 observed versus OOB prediction plot (Figure 5) depicted some decrease in yield, which we noted
347 varied as a function of elevation.

348 3.4. Predictor variable importance

349 The most important predictors in the final model (Figure 6) included the stationary variables of
350 elevation, nitrogen, and cec, since without accounting for them, the prediction error (OOB MSE)
351 would increase by 14, 11 and $10 t.ha^{-1}$, respectively. Temporal variables `ndvi_07-03`, `ppt_07-19` and
352 `tmin_06-01` were also deemed important, as permuting each of them resulted in an error of 9.7, 8.7 and
353 $7.5 t.ha^{-1}$, respectively. The variable `ndvi_07-03` represented the vegetation greenness in sweetpotato

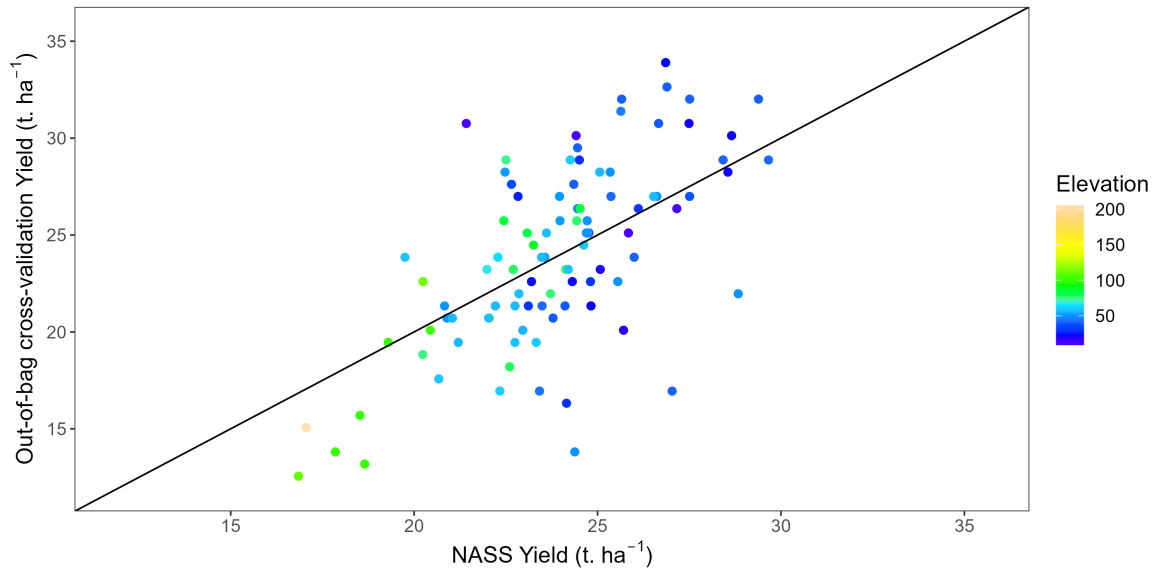


Figure 5: NASS county yields (USDA National Agricultural Statistics Service, 2022b) versus out-of-bag predictions from the final model. Dots are colored by the most important variable, elevation (m.)

354 pixels within a county during the first month of the growing season, which is the critical stage
 355 for storage root initiation. The variable ppt_07-19 was the amount of precipitation during storage
 356 bulking, which also influences final yield (Gajanayake and Reddy, 2016). And, tmin_06-01 included
 357 the minimum temperature around planting and establishment, also a critical stage.

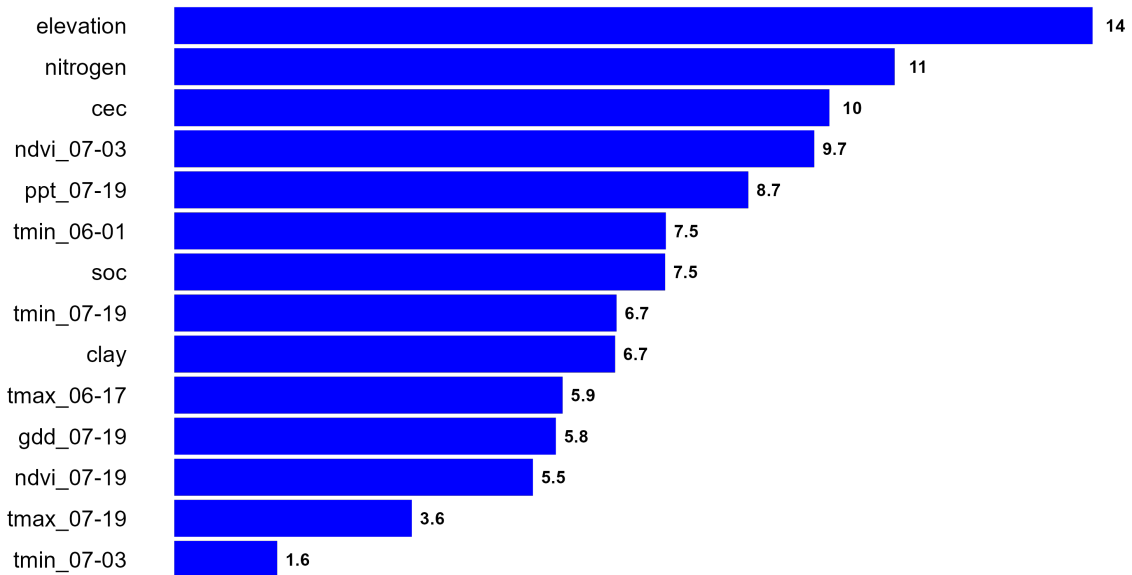


Figure 6: Importance of predictors determined by the Random Forest model (RFR) for sweetpotato yield forecasting at county-level. The RFR model was built with stationary and early to mid season predictors and 16-day composites for temporally variant predictors. Importance is defined as the increase in the MSE prediction when the variables is permuted (e.g. 14 for elevation)

358 Figure 7 depicts the variability of the variables included in the final RFR model and the target
 359 variable. While the response variable, yield, ranged from 12.55 to 33.89 $t.ha^{-1}$ without outliers,
 360 some predictors (e.g., elevation, soc and gdd.07-19) had low spatial variation, with some outliers.

361 Unsurprisingly, since high production areas for sweetpotato in North Carolina are primarily situated
362 in the Coastal Plains, with elevations gradually increasing towards the northeast, county elevations
363 ranged from 9 to 205 meters above sea level (m.a.s.l.), with approximately 50% of the data falling
364 within the range of 39 to 60 m.a.s.l. In contrast, nitrogen and cec at 5-15 cm depth ranged from
365 0.78 to 1.70 $g.kg^{-1}$ and from 6.4 to 16.3 $cmol_c.kg^{-1}$, respectively, had a more balanced distribution
366 with only a few superior outliers. The cec values were distributed across the typical values for fine
367 sandy loam and loam soil, with low to medium organic matter and water holding capacity. NDVI
368 values after storage root initiation (ndvi_07-03) ranged from 0.19 to 0.81; however, 50% of data ranged
369 only from 0.39 to 0.53, which means that vegetation coverage was about the same. Similarly, total
370 precipitation during the period of greatest storage root bulking (ppt_07-19), ranged from 4.58 to
371 197.19 mm., showing the high variability of rain even within a relatively small productive region.
372 Minimum temperature just after planting mostly varied from 18.76 to 19.85 °C (tmin_06-01), with a
373 few minimum outliers down to 14.82 °C.

374 4. Discussion

375 When screening candidate predictor variables, we found that the stationary variables of elevation,
376 nitrogen, and cec consistently had the highest importance, and soc and clay to a lesser extent (Figure
377 4. In the final model built with RFR, the stationary variables had the greatest effect on sweetpotato
378 yield predictions at the county scale. Elevation was the most important predictor variable; however, it
379 should be interpreted as an indicator of the geographic location in NC, since sweetpotatoes are grown
380 in a region with flat terrain. Similarly, when considering the factors that influence soil formation
381 across the state, elevation emerges as the most influential element, significantly shaping the definition
382 of soil units and, consequently, their characteristics (Lee, 1955). Thus, elevation is most likely acting
383 as a proxy for other geospatial covariates such as soil quality and climate patterns, which spatially
384 and temporally determine the sweetpotato growth. As a result, these factors make certain regions
385 more suitable for sweetpotato cultivation, leading to the development of more advanced management
386 practices, and consequently, achieving high yields. With regards to the importance of nitrogen, since
387 it represents the total nitrogen in the soil rather than the nitrogen fertilizer applied or available
388 to the plants, it is likely a proxy for soil drainage quality. Well-drained soils often require more
389 nitrogen application due to leaching. These soils typically are sandy textures, which are preferred
390 by sweetpotatoes due to the ample pore spaces that facilitate storage root growth. Finally, cec's
391 importance reflects its role in indicating soil type and health, as soils with higher cec are better at
392 retaining essential nutrients (Kaiser et al., 2008), directly correlating with the optimal growth and
393 yield of sweetpotatoes in NC's diverse agricultural systems. The predominant importance of elevation
394 and soil properties (stationary variables) over weather or vegetation indexes (temporal variables) is

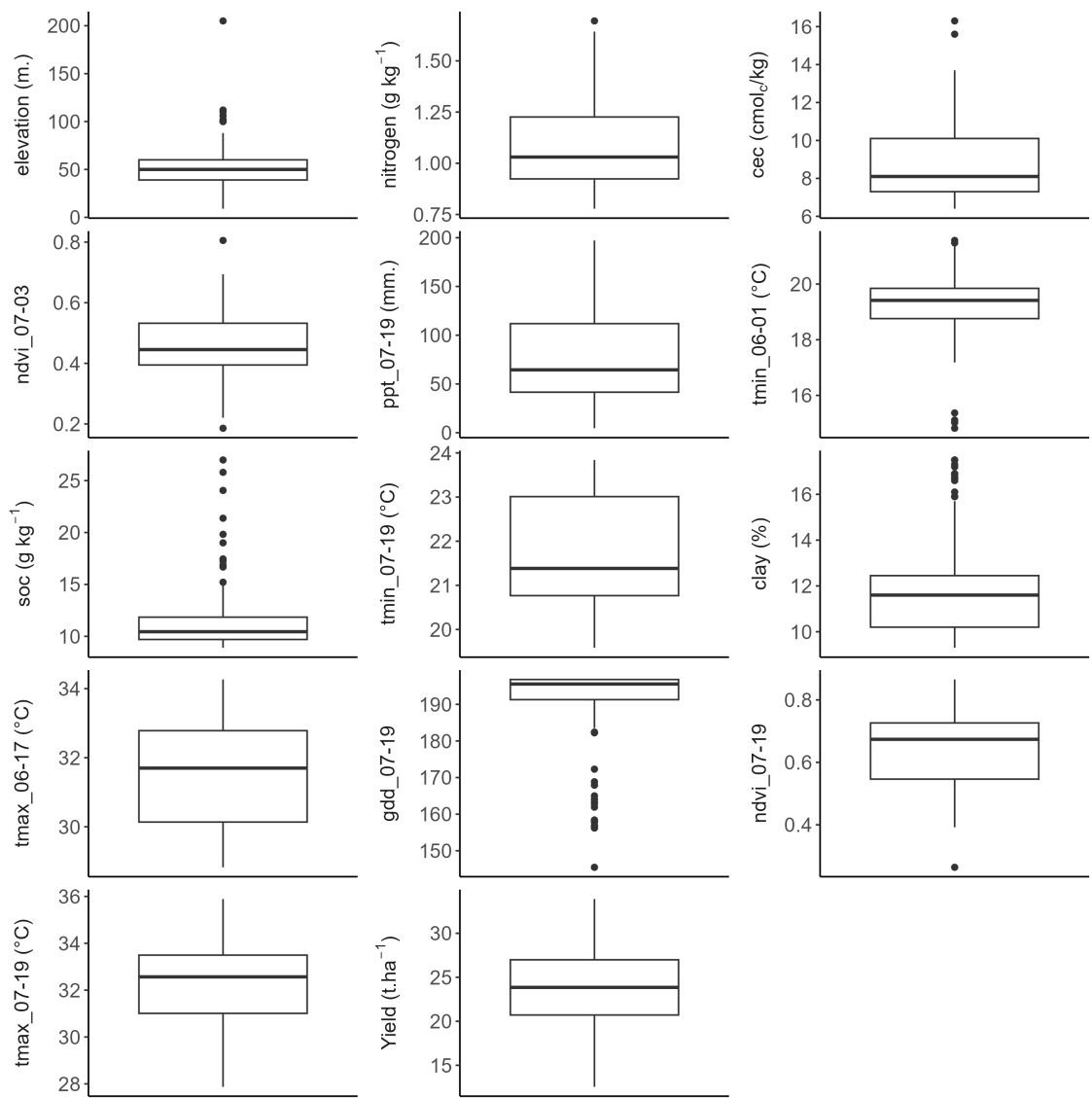


Figure 7: Boxplot showing the variability of all-relevant variables selected after Boruta feature selection

395 supported by previous studies such as Cao et al. (2021), where elevation had significant correlations
396 between climate factors when modeling wheat yield for thirteen China’s provinces.

397 In contrast to stationary predictors, temporal variables were less consistently important, particu-
398 larly when data across multiple growing season stages (i.e., early-mid, early-late) were considered. In
399 the final RFR model, which only considered measurements of temporally-varying predictors from the
400 early and mid growing season, temporal input variables `ndvi_07-03`, `ppt_07-19`, and `tmin_06-01` were
401 the most important temporally variant predictors. The importance of `ndvi_07-03`, the 16-day NDVI
402 composite starting on July 03, the 4th most important variable, indicates that canopy growth is an
403 important predictor of end-of-season yields. The importance of NDVI in the early and mid-growing
404 season as a yield predictor is corroborated by prior research demonstrating that early and mid-canopy
405 growth is correlated with root development (Tedesco et al., 2021). Variable `ppt_07-19`, the 5th most
406 important variable, represented the total precipitation in the mid-season, which is a critical time for
407 storage root bulking and the end-season yield (Gajanayake and Reddy, 2016), with some variability
408 across regions in NC (Zarzar and Dyer, 2019). Finally, `tmin_06-01`, the 6th most important variable,
409 is the mean minimum temperature in the early growing season near transplanting. Because average
410 temperatures need to be greater than 16.8 ° for successful sweetpotato transplanting and root estab-
411 lishment (Gajanayake et al., 2014), the inclusion of this predictor in the final model captures a known
412 mechanism driving sweetpotato growth and yields. Overall, the predictor variables and the associ-
413 ated timing of the predictors included in the final model correspond to established environmental
414 relationships known to affect sweetpotato productivity.

415 Though the RFR algorithm with 16-day composite predictors spanning the early and mid-growing
416 season was selected as the best and final model, other ML algorithms and predictor composite pe-
417 riods were considered. RFR outperformed the other ML algorithms (ANN, SVM and XGB) and its
418 evaluation metrics were the most consistent across the six considered predictor sets, especially when
419 both mid and late-season temporal variables were included as predictors. Models with 16- and 32-day
420 composite and only early season data had slightly lower performances. This suggests that having nu-
421 merous temporal variable predictors was not necessarily advantageous; instead, the composited data
422 may have introduced noise into the model, diminishing its robustness. The final model’s performance
423 was moderate (testing: $R^2 = 0.44$, $RMSE = 3.53 \text{ t.ha}^{-1}$), and considered acceptable for forecasting
424 given that the models predict how sweetpotato yield will vary as a function of environmental con-
425 ditions alone. To improve model performance, predictors capturing other drivers that affect actual
426 yield (e.g., genotype characteristics and management practices) should be included. Future work
427 could build upon the regional models presented here to provide more tailored forecast products for
428 individual farms.

429 Interestingly, models that included predictors from the late growing season did not outperform

430 the models that only considered temporally varying predictors from the early and mid-season. The
431 inclusion of late-season predictors was expected to result in more accurate forecasts since conditions
432 late in the growing season (e.g., NDVI near harvest) were expected to more closely correlate with final
433 yields. Yet, the testing R^2 for the RFR model with 16-day composites and early-late season predictors
434 was 0.44, and the equivalent model with early-mid season predictors was also 0.44, indicating the late
435 season values did not improve model performance. However, the testing R^2 for the RFR model with
436 16-day composites that only included early season predictors was 0.36. These results indicate that
437 environmental conditions spanning the early and mid-season are predictive of yields at harvest, and
438 that information from later in the season is not necessary to boost performance. Operationally, these
439 findings demonstrate that the best time to run this forecast model is at the end of the mid-season,
440 approximately between four to eight weeks before harvest. However, depending on end-user interests,
441 the RFR model with 16-day composites using only early season values for temporal predictors (i.e.,
442 the model with a testing R^2 of 0.36) may be more desirable despite its poorer performance, as it
443 could be run as early as eight to twelve weeks before harvest.

444 While our results demonstrate an in-season yield forecasting model for sweetpotato performs rea-
445 sonably well and can provide actionable information, there are opportunities to further expand the
446 frameworks tested here. For example, Zhou et al. (2022) found that solar-induced chlorophyll fluo-
447 rescence (SIF) had better predictability for yield than traditional vegetation indices, so the inclusion
448 of SIF could potentially improve model performance. Similarly, previous studies reported superior
449 predictive power from Land Surface Temperature (LST) over air temperature given it provides in-
450 formation on canopy temperature, which is related to water and heat stresses (Kang et al., 2020;
451 Siebert, Stefan and Ewert, Frank and Rezaei, Ehsan Eyshi and Kage, Henning and Graß, Rikard,
452 2014; Pede et al., 2019). Although deep learning (DL) algorithms, such as Long Short-Term Mem-
453 ory (Van Klompenburg et al., 2020), have shown promise in yield forecasting at county scale, they
454 typically require larger datasets. Furthermore, a prior study comparing DL and traditional machine
455 learning (ML) algorithms found that DL algorithms did not demonstrate superior performance over
456 ML models like Random Forest or Extreme Gradient Boosting at the county scale (Kang et al., 2020;
457 Cao et al., 2021).

458 The most significant limitation of this study stemmed from the small sample size, which was
459 a result of the restricted availability of yield data for sweetpotatoes, thereby constraining the ML
460 process and its overall robustness. Additionally, at the county level, spatial error and uncertainties
461 were inevitably introduced to the model during data preprocessing, particularly when compositing
462 temporal data and matching coarse spatial data of varying resolution. Moreover, as demonstrated by
463 the comparison of sweetpotato harvested areas from USDA CDL, Survey, and Census data (Figure
464 3 and Table 4), there are uncertainties even in the locations of farms, and the reliance on farmer-

465 reported yields results in the sweetpotato yield data being affected by survey participation rates
466 and respondent honesty. Additionally, while satellite image inputs and classification methods have
467 led to improved CDL accuracy over time, the CDL’s accuracy has only been tested for select crops
468 and regions; prior research shows that CDL performs best for major crops (producer’s accuracies
469 of 71.5%), aggregated categories, and within major cropping regions such as the Corn Belt, Central
470 Plains, and Mississippi Delta (Lark et al., 2021). Regardless, CDL demonstrated good county-scale
471 agreement with Census and Survey data (Table 4), and was considered a good source for identifying
472 sweetpotato fields since it is able to estimate field locations that may be hidden from NASS survey
473 data in an effort to protect grower identity. NASS safeguards individual farm privacy by excluding
474 farms from reporting if they have fewer than 100 planted acres, and about 50% of farms in North
475 Carolina are between 1 to 49 acres (0.4 - 19.8 *ha*) (U.S. Department of Agriculture, 2022).

476 **5. Conclusions**

477 This study analyzed four ML algorithms for predicting sweetpotato yield using stationary and
478 temporal environmental variables as potential predictors. The six predictor sets, which varied in the
479 amount of in-season data they considered as well as the aggregation period of temporal variables
480 (16- vs 32-day), provided key information about important variables and models’ performance. In
481 particular, elevation, which is an indicator of geographic location, had the highest importance. The
482 RFR model consistently outperformed the other ML algorithms. We determined that the best model
483 configuration for temporal variables used early and mid-season data with 16-day composited tempo-
484 ral variables. Using late-season data did not improve model performance. Among the various input
485 variables considered, the stationary ones (elevation, nitrogen and cec), followed by NDVI and precip-
486 itation after storage root initiation and bulking (July), and minimum temperature around planting
487 (June), were the most predictive of sweetpotato yield at the county scale.

488 Publicly available in-season remote sensing data, coupled with machine learning models, can
489 predict sweetpotato yields reasonably well before the season’s end. This approach aims to aid growers
490 in enhancing their harvest management, optimizing marketable yield, planning storage, refining sales
491 and marketing strategies, and even plan for the next year’s planting. Furthermore, it provides valuable
492 insights to decision-makers, facilitating more accurate estimates of crop insurance payments, revenue
493 support programs, and collaborative planning with local extension agents and agribusinesses.

494 **Acknowledgements**

495 This work was supported by USDA NIFA project 2019-67021-29936, grant (1404) 2020–1160
496 through North Carolina State University’s Plant Sciences Initiative (NC PSI) Game-Changing Re-
497 search Incentive Program, and USDA NIFA Hatch project 7003506.

498 **References**

- 499 Abbas, F., Afzaal, H., Farooque, A.A., Tang, S., 2020. Crop yield prediction through proximal sensing
500 and machine learning algorithms. *Agronomy* 10, 1046.
- 501 Ahsan, M.M., Mahmud, M.P., Saha, P.K., Gupta, K.D., Siddique, Z., 2021. Effect of data scaling
502 methods on machine learning algorithms and model performance. *Technologies* 9, 52.
- 503 Balabaeva, K., Kovalchuk, S., 2019. Comparison of temporal and non-temporal features effect on
504 machine learning models quality and interpretability for chronic heart failure patients. *Procedia*
505 *Computer Science* 156, 87–96.
- 506 Cao, J., Zhang, Z., Luo, Y., Zhang, L., Zhang, J., Li, Z., Tao, F., 2021. Wheat yield predictions at
507 a county and field scale with deep learning, machine learning, and google earth engine. *European*
508 *Journal of Agronomy* 123, 126204.
- 509 Chastain, R., Housman, I., Goldstein, J., Finco, M., Tenneson, K., 2019. Empirical cross sensor
510 comparison of sentinel-2a and 2b msi, landsat-8 oli, and landsat-7 etm+ top of atmosphere spectral
511 characteristics over the conterminous united states. *Remote sensing of environment* 221, 274–285.
- 512 Chen, T., Guestrin, C., 2016. XGBoost: A scalable tree boosting system, in: *Proceedings of the 22nd*
513 *ACM SIGKDD International Conference on Knowledge Discovery and Data Mining*, ACM, New
514 York, NY, USA. pp. 785–794. URL: <http://doi.acm.org/10.1145/2939672.2939785>, doi:10.
515 1145/2939672.2939785.
- 516 Chicco, D., Warrens, M.J., Jurman, G., 2021. The coefficient of determination r-squared is more in-
517 formative than smape, mae, mape, mse and rmse in regression analysis evaluation. *PeerJ Computer*
518 *Science* 7, e623.
- 519 Dufault, R.J., 1997. Determining Heat Unit Requirements for Broccoli Harvest in Coastal South
520 Carolina. *Journal of the American Society for Horticultural Science* 122, 169–174. doi:10.21273/
521 *JASHS.122.2.169*. publisher: American Society for Horticultural Science Section: Journal of the
522 American Society for Horticultural Science.
- 523 Fei, S., Li, L., Han, Z., Chen, Z., Xiao, Y., 2022. Combining novel feature selection strategy and
524 hyperspectral vegetation indices to predict crop yield. *Plant Methods* 18, 1–13.
- 525 Gajanayake, B., Reddy, K.R., 2016. Sweetpotato responses to mid-and late-season soil moisture
526 deficits. *Crop Science* 56, 1865–1877.
- 527 Gajanayake, B., Reddy, K.R., Shankle, M.W., Arancibia, R.A., Villordon, A.O., 2014.
528 Quantifying Storage Root Initiation, Growth, and Developmental Responses of Sweet-
529 potato to Early Season Temperature. *Agronomy Journal* 106, 1795–1804. URL: [https:](https://doi.org/10.1007/s12230-014-9548-4)

530 [//onlinelibrary.wiley.com/doi/abs/10.2134/agronj14.0067](https://onlinelibrary.wiley.com/doi/abs/10.2134/agronj14.0067), doi:10.2134/agronj14.0067.
531 eprint: <https://access.onlinelibrary.wiley.com/doi/pdf/10.2134/agronj14.0067>.

532 Ghazaryan, G., Skakun, S., König, S., Rezaei, E.E., Siebert, S., Dubovyk, O., 2020. Crop yield
533 estimation using multi-source satellite image series and deep learning, in: IGARSS 2020-2020
534 IEEE International Geoscience and Remote Sensing Symposium, IEEE. pp. 5163–5166.

535 Gómez, D., Salvador, P., Sanz, J., Casanova, J.L., 2019. Potato yield prediction using machine
536 learning techniques and sentinel 2 data. *Remote Sensing* 11, 1745.

537 Griffith, G.E., Omernik, J.M., Comstock, J., Schafale, M., McNab, W., Lenat, D., MacPherson, T.,
538 2002. Ecoregions of North Carolina. Western Ecology Division, National Health and Environmental
539 Effects Research

540 Jarvis, A., Reuter, H.I., Nelson, A., Guevara, E., et al., 2008. Hole-filled srtm for the globe version
541 4. available from the CGIAR-CSI SRTM 90m Database (<http://srtm.csi.cgiar.org>) 15, 5.

542 Jung, J., Maeda, M., Chang, A., Bhandari, M., Ashapure, A., Landivar-Bowles, J., 2021. The
543 potential of remote sensing and artificial intelligence as tools to improve the resilience of agriculture
544 production systems. *Current Opinion in Biotechnology* 70, 15–22.

545 Kaiser, M., Ellerbrock, R., Gerke, H., 2008. Cation exchange capacity and composition of soluble soil
546 organic matter fractions. *Soil Science Society of America Journal* 72, 1278–1285.

547 Kang, Y., Ozdogan, M., Zhu, X., Ye, Z., Hain, C., Anderson, M., 2020. Comparative assessment
548 of environmental variables and machine learning algorithms for maize yield prediction in the us
549 midwest. *Environmental Research Letters* 15, 064005.

550 Keskin, H., Grunwald, S., Harris, W.G., 2019. Digital mapping of soil carbon fractions with machine
551 learning. *Geoderma* 339, 40–58.

552 Khan, N.M., Madhav C., N., Negi, A., Thaseen, I.S., 2020. Analysis on improving the performance
553 of machine learning models using feature selection technique, in: *Intelligent Systems Design and
554 Applications: 18th International Conference on Intelligent Systems Design and Applications (ISDA
555 2018) held in Vellore, India, December 6-8, 2018, Volume 2*, Springer. pp. 69–77.

556 Kuhn, Max, 2008. Building predictive models in r using the caret package. *Journal of Statistical
557 Software* 28, 1–26. URL: <https://www.jstatsoft.org/index.php/jss/article/view/v028i05>,
558 doi:10.18637/jss.v028.i05.

559 Kursa, M.B., Jankowski, A., Rudnicki, W.R., 2010. Boruta—a system for feature selection. *Funda-
560 menta Informaticae* 101, 271–285.

561 Kursa, M.B., Rudnicki, W.R., 2010. Feature selection with the Boruta package. *Journal of Statistical*
562 *Software* 36, 1–13. URL: <https://doi.org/10.18637/jss.v036.i11>.

563 Lark, T.J., Schelly, I.H., Gibbs, H.K., 2021. Accuracy, bias, and improvements in mapping crops and
564 cropland across the united states using the usda cropland data layer. *Remote Sensing* 13, 968.

565 Lee, W.D., 1955. *The Soils of North Carolina: Their Formation, Identification and Use*. 115, North
566 Carolina Agricultural Experiment Station.

567 Leng, G., Hall, J.W., 2020. Predicting spatial and temporal variability in crop yields: an inter-
568 comparison of machine learning, regression and process-based models. *Environmental Research*
569 *Letters* 15, 044027.

570 Li, D., Miao, Y., Gupta, S.K., Rosen, C.J., Yuan, F., Wang, C., Wang, L., Huang, Y., 2021. Improv-
571 ing potato yield prediction by combining cultivar information and uav remote sensing data using
572 machine learning. *Remote Sensing* 13, 3322.

573 Liaw, A., Wiener, M., 2002. Classification and regression by randomforest. *R News* 2, 18–22. URL:
574 <https://CRAN.R-project.org/doc/Rnews/>.

575 Meyers, S.L., Jennings, K.M., Monks, D.W., 2014. ‘covington’sweetpotato tolerance to flumioxazin
576 applied post-directed. *Weed Technology* 28, 163–167.

577 NC State Extension, 2017. North carolina sweet potatoes. URL: [https://lee.ces.ncsu.edu/2017/](https://lee.ces.ncsu.edu/2017/12/north-carolina-sweet-potatoes/)
578 [12/north-carolina-sweet-potatoes/](https://lee.ces.ncsu.edu/2017/12/north-carolina-sweet-potatoes/). accessed on October 02, 2023.

579 Paudel, D., Boogaard, H., de Wit, A., van der Velde, M., Claverie, M., Nisini, L., Janssen, S., Osinga,
580 S., Athanasiadis, I.N., 2022. Machine learning for regional crop yield forecasting in europe. *Field*
581 *Crops Research* 276, 108377.

582 Pede, T., Mountrakis, G., Shaw, S.B., 2019. Improving Corn Yield Prediction Across the U.S. Corn
583 Belt by Replacing Air Temperature with Daily MODIS Land Surface Temperature. *Agricultural*
584 *and Forest Meteorology* 276, 107615.

585 Pérez-Pazos, J.V., Rosero, A., Martínez, R., Pérez, J., Morelo, J., Araujo, H., Burbano-Erazo, E.,
586 2021. Influence of morpho-physiological traits on root yield in sweet potato (*ipomoea batatas lam.*)
587 genotypes and its adaptation in a sub-humid environment. *Scientia Horticulturae* 275, 109703.

588 Poggio, L., De Sousa, L.M., Batjes, N.H., Heuvelink, G., Kempen, B., Ribeiro, E., Rossiter, D., 2021.
589 *Soilgrids 2.0: producing soil information for the globe with quantified spatial uncertainty. Soil* 7,
590 217–240.

591 PRISM Climate Group, Oregon State University, 2022. <https://prism.oregonstate.edu>. URL: <https://prism.oregonstate.edu>. accessed on September 26, 2023.

592

593 R Core Team, 2023. R: A Language and Environment for Statistical Computing. R Foundation for
594 Statistical Computing. Vienna, Austria. URL: <https://www.R-project.org/>.

595 Roy, D.P., Kovalskyy, V., Zhang, H., Vermote, E.F., Yan, L., Kumar, S., Egorov, A., 2016. Char-
596 acterization of landsat-7 to landsat-8 reflective wavelength and normalized difference vegetation
597 index continuity. *Remote sensing of Environment* 185, 57–70.

598 RStudio Team, 2021. RStudio: Integrated Development Environment for R. RStudio, PBC. Boston,
599 MA. URL: <http://www.rstudio.com/>.

600 Salvador, P., Gómez, D., Sanz, J., Casanova, J.L., 2020. Estimation of potato yield using satellite
601 data at a municipal level: A machine learning approach. *ISPRS International Journal of Geo-*
602 *Information* 9, 343.

603 Siebert, Stefan and Ewert, Frank and Rezaei, Ehsan Eyshi and Kage, Henning and Graß, Rikard, 2014.
604 Impact of Heat Stress on Crop Yield—On the Importance of Considering Canopy Temperature.
605 *Environmental Research Letters* 9, 044012.

606 Soto-Caro, A., Luo, T., Wu, F., Guan, Z., 2022. The U.S. sweet potato market: Price response and
607 impact of supply shocks. *Horticulturae* 8, 856.

608 Strobl, C., Boulesteix, A.L., Zeileis, A., Hothorn, T., 2007. Bias in random forest variable importance
609 measures: Illustrations, sources and a solution. *BMC bioinformatics* 8, 1–21.

610 Sun, C., Feng, L., Zhang, Z., Ma, Y., Crosby, T., Naber, M., Wang, Y., 2020. Prediction of end-of-
611 season tuber yield and tuber set in potatoes using in-season uav-based hyperspectral imagery and
612 machine learning. *Sensors* 20, 5293.

613 Tedesco, D., de Oliveira, M.F., dos Santos, A.F., Silva, E.H.C., de Souza Rolim, G., da Silva, R.P.,
614 2021. Use of remote sensing to characterize the phenological development and to predict sweet
615 potato yield in two growing seasons. *European Journal of Agronomy* 129, 126337.

616 Togari, Y., 1950. A study in the tuberous-root formation of sweet potato. *Bull. Natl. Agric. Exp.*
617 *Stn.* 68, 1–96.

618 U.S. Department of Agriculture, 2022. North carolina annual statistical bulletin highlights. URL:
619 [https://www.nass.usda.gov/Statistics_by_State/North_Carolina/Publications/Annual_](https://www.nass.usda.gov/Statistics_by_State/North_Carolina/Publications/Annual_Statistical_Bulletin/AgStat/NCHighlights.pdf)
620 [Statistical_Bulletin/AgStat/NCHighlights.pdf](https://www.nass.usda.gov/Statistics_by_State/North_Carolina/Publications/Annual_Statistical_Bulletin/AgStat/NCHighlights.pdf). accessed on October 9, 2023.

621 U.S. Geological Survey, 2023. How do i use a scale factor in landsat level-2 science products? <https://www.usgs.gov/faqs/how-do-i-use-a-scale-factor-landsat-level-2-science-products>.
622
623 Accessed on September 26, 2023.

624 USDA National Agricultural Statistics Service, 2022a. Cropland data layer (2008 - 2022). published
625 crop-specific data layer. URL: <https://nassgeodata.gmu.edu/CropScape/>. accessed on Septem-
626 ber 26, 2023.

627 USDA National Agricultural Statistics Service, 2022b. NASS - Quick Stats. <https://data.nal.usda.gov/dataset/nass-quick-stats>. Accessed on September 27, 2023.
628

629 Van Klompenburg, T., Kassahun, A., Catal, C., 2020. Crop yield prediction using machine learning:
630 A systematic literature review. *Computers and Electronics in Agriculture* 177, 105709.

631 Venables, W.N., Ripley, B.D., 2002. *Modern Applied Statistics with S*. Fourth ed., Springer, New
632 York. URL: <https://www.stats.ox.ac.uk/pub/MASS4/>. iISBN 0-387-95457-0.

633 Villaescusa-Nadal, J.L., Franch, B., Roger, J.C., Vermote, E.F., Skakun, S., Justice, C., 2019. Spectral
634 adjustment model's analysis and application to remote sensing data. *IEEE Journal of Selected*
635 *Topics in Applied Earth Observations and Remote Sensing* 12, 961–972.

636 Villordon, A., Clark, C., Ferrin, D., LaBonte, D., 2009a. Using Growing Degree Days,
637 Agrometeorological Variables, Linear Regression, and Data Mining Methods to Help Im-
638 prove Prediction of Sweetpotato Harvest Date in Louisiana. *HortTechnology* 19, 133–144.
639 URL: <https://journals.ashs.org/horttech/view/journals/horttech/19/1/article-p133.xml>, doi:10.21273/HORTSCI.19.1.133. publisher: American Society for Horticultural Science Sec-
640 tion: HortTechnology.

641

642 Villordon, A., LaBonte, D., Firon, N., 2009b. Development of a simple thermal time method for
643 describing the onset of morpho-anatomical features related to sweetpotato storage root formation.
644 *Scientia horticultrae* 121, 374–377.

645 Villordon, A., Sheffield, R., Rojas, J., Chiu, Y.L., 2011. Development of simple bayesian belief
646 and decision networks as interactive visualization tools for determining optimal in-row spacing for
647 'beauregard'sweetpotato. *HortScience* 46, 1588–1597.

648 Villordon, A., Solis, J., LaBonte, D., Clark, C., 2010. Development of a prototype bayesian network
649 model representing the relationship between fresh market yield and some agroclimatic variables
650 known to influence storage root initiation in sweetpotato. *HortScience* 45, 1167–1177.

651 Yenko, G.C., Pecota, K.V., Schultheis, J.R., VanEsbroeck, Z.P., Holmes, G.J., Little, B.E., Thorn-
652 ton, A.C., Truong, V.D., 2008. 'covington'sweetpotato. *HortScience* 43, 1911–1914.

- 653 Yin, F., Lewis, P.E., Gomez-Dans, J.L., Wu, Q., 2019. A sensor-invariant atmospheric correction
654 method: Application to Sentinel-2/MSI and Landsat 8/OLI. Preprint .
- 655 Zarzar, C., Dyer, J., 2019. The influence of synoptic-scale air mass conditions on seasonal precipitation
656 patterns over North Carolina. *Atmosphere* 10, 624.
- 657 Zhang, H.K., Roy, D.P., Yan, L., Li, Z., Huang, H., Vermote, E., Skakun, S., Roger, J.C., 2018.
658 Characterization of sentinel-2a and landsat-8 top of atmosphere, surface, and nadir brdf adjusted
659 reflectance and ndvi differences. *Remote sensing of environment* 215, 482–494.
- 660 Zhou, W., Liu, Y., Ata-Ul-Karim, S.T., Ge, Q., Li, X., Xiao, J., 2022. Integrating climate and
661 satellite remote sensing data for predicting county-level wheat yield in china using machine learning
662 methods. *International Journal of Applied Earth Observation and Geoinformation* 111, 102861.